ORIGINAL ARTICLE

Phylogenomics, biogeography, and evolution in the American palm genus *Brahea*

Craig F. Barrett[1,*], Brandon T. Sinn[1], Loren T. King[1], Jesus C. Medina[2], Christine D. Bacon[3,4], Sean C. Lahmeyer[5], and Donald R. Hodel[6]

[1]Department of Biology, West Virginia University, 53 Campus Dr., Morgantown, West Virginia, USA 26506

[2]Department of Biological Sciences, California State University, 5151 State University Dr., Los Angeles, Los Angeles, California, USA 90032

[3]Department of Biological and Environmental Sciences, University of Gothenburg, Carl Skottsbergs gata 22B, P.O. Box 461, SE 405 30, Göteborg, Sweden

[4]Gothenburg Global Biodiversity Centre, Box 461, SE-405 30, Göteborg, Sweden

[5]The Huntington Library, Art Collections, and Botanical Gardens, 1151 Oxford Road, San Marino, California, USA 91108

[6]University of California Cooperative Extension, 700 West Main Street, Alhambra, California USA 91801

*Corresponding author. Email: cfb0001@mail.wvu.edu, phone: 1 (304) 293-7506

ABSTRACT

- **Background and Aims**: Slow rates of molecular evolution at low taxonomic levels hamper studies of relationships among species, and subsequent biogeographic and evolutionary analyses. An example is the genus *Brahea*, which is among the most poorly understood lineages of American palms and is characterized by a wide variety of growth forms and intermediate morphological features.
- **Methods**: We generated approximately 400 kb of genome-scale data from all three genomes for the 11 currently described species of *Brahea* to infer phylogenetic relationships, reconstruct ancestral growth form, estimate ancestral geographic ranges, and test for niche equivalency among closely related species with geographic overlap.
- **Key Results**: Relationships receive strong support, and conform to previous subgeneric assignments, except for placement of the dwarf species *B. moorei* within subgenus *Erythea*. Our robust phylogenetic hypothesis reveals trends in growth form including an overall increase in height in the *B. armata* clade, and independent evolution of dwarf forms from taller ancestors in the *B. pimo* and *B. dulcis* clades. Ancestral range estimation reveals roles of dispersal (e.g. *B. edulis* on Guadalupe Island) and sympatric speciation in some cases (e.g. in the *B. armata* clade), but is equivocal in others (e.g. in the *B. pimo clade*). We find evidence of niche non-equivalency among species within the *B. armata* clade in northwestern Mexico, and some evidence of niche non-equivalency between *B. berlandieri* and *B. dulcis*, the former of which is synonymized under *B. dulcis*.
- **Conclusions**: Our findings have implications for the complex biogeographic history in Central America and Mexico, suggesting that sympatric speciation and dispersal are the predominant processes of species diversification. Future studies should include population-level sampling across the genus, along with morphological and ecological information, to assess distinctness among species and, particularly, levels of gene flow, in an integrative fashion.

KEY WORDS

Central America, diversification, growth forms, Mexico, niche, phylogeny, Arecaceae

INTRODUCTION

The palms (family Arecaceae) are globally emblematic components of tropical and subtropical ecosystems (Uhl and Drandfield, 1987; Dransfield, Uhl, *et al.*, 2008; Asmussen *et al.*, 2006; Baker *et al.*, 2009; Baker and Dransfield, 2016; Balslev et al., 2016). Palms are notorious for having slow substitution rates among the monocot angiosperms, likely resulting from their large size and associated consequences for the inheritance of new mutations (Gaut *et al.*, 1992; Lanfear *et al.*, 2013; Barrett *et al.*, 2016a). Slow mutation rates equate to fewer informative molecular characters for phylogenetic analysis, and thus hamper our understanding of interspecific relationships in many clades. Resolved, strongly supported phylogenetic hypotheses form an essential basis for taxonomic research and subsequent inference of character evolution, biogeography, and niche evolution. Genome-scale datasets provide a solution, having become feasible to obtain with the widespread availability of high-throughput sequencing methods. Not surprisingly, palm systematists have begun to embrace phylogenomic approaches (Comer *et al.*, 2015; Barrett *et al.*, 2016a; Comer *et al.*, 2016; Barrett *et al.*, 2016b; Heyduk *et al.*, 2016; Bacon *et al.* in review).

The fan palm genus *Brahea* Endl. *ex* Mart. exemplifies the situation described above, and is among the most taxonomically problematic and poorly understood clades of American palms (subfamily Coryphoideae, tribe Trachycarpeae, within which the placement of *Brahea* is uncertain; Quero and Yáñez, 2000; Quero, 2000; Hodel, 2006; Dransfield et al., 2008; Bacon *et al.*, 2012; Barrett et al., 2015; Baker and Dransfield, 2016). The genus comprises 11 currently recognized species (Hodel, 2006; Govaerts et al., 2018), that grow in dry, often calcareous soils in the coastal and lower montane regions of Mexico and Central America extending to Nicaragua. *Brahea* sometimes occurs with *Sabal* and *Washingtonia*, two other fan palm genera. The costapalmate leaf blades (i.e. extension of petiole into the blade) distinguish *Sabal* from *Brahea*. *Washingtonia*, which occurs natively in Baja California and Sonora, Mexico and in isolated oases in California and Arizona (and perhaps Nevada?), USA, has a similar overall appearance to some *Brahea* species, but differs in its bright to dull green leaves, whereas co-occuring *Brahea* (*B. armata, B. brandegeei*) have blue-green or gray leaves. Florally *Brahea* has three carpels connate only in the styles while *Sabal* has three carpels connate throughout. *Brahea* has tubular inflorescence rachis bracts while those of *Washingtonia* split on one side, become pendulous and are sword shaped.

Endlicher (1837) first informally used the genus name *Brahea*, honoring the Danish astronomer Tycho Brahe, and Martius (1838) validly published it a year later. Watson (1880) subsequently described the genus *Erythea*, which contains some species currently recognized in *Brahea*. *Brahea* was originally distinguished as having unarmed petioles, relatively small fruits, and solitary flowers, whereas *Erythea* was distinguished by having armed petioles, larger fruits, and clustered flowers at the base of the inflorescence. Moore (1973) and Uhl and Dransfield (1987) recognized these genera as a single genus, *Brahea*, with two subgenera—*Brahea* and *Erythea*. More recently, Quero and Yáñez (2000), and subsequently Hodel (2006) have refined

various names associated with *Brahea* into 12 and 11 species, respectively, based on morphological and ecological observations. While other treatments recognize nine species (e.g. Henderson et al. 1995), here we follow Hodel (2006, see also Hodel 2018) and Govaerts et al. (2018) the most recent and comprehensive treatments of the genus.

Subgenus *Erythea*, as currently circumscribed, contains seven species. *Brahea aculeata*, *B. armata*, and *B. brandegeei* are found in the arid, desert scrub regions of northwestern Mexico and Baja California, and are distinguished by having distinctly armed petioles. *Brahea edulis* is endemic to Guadalupe Island, located approximately 240 km west of Baja California, and is IUCN red-listed as endangered in the wild (EN, C1; Johnson, 1998). This species is distinguished by unarmed petioles and large fruit size (> 25 mm in diameter). *Brahea pimo* occurs in the western pine-oak sierras of Mexico, and *B. salvadorensis* is restricted to El Salvador and Guatemala. These two species have distinctive hairy scales on the petioles and adaxial leaf surfaces and hairy-tomentose flowers, differing mainly in the degree of the latter.

Subgenus *Brahea* contains the widespread and highly variable *B. dulcis* and *B. calcarea* from Mexico into Guatemala, Honduras, and Nicaragua. The subgenus is distinguished mainly by absence or reduction of petiolar teeth. *Brahea dulcis* has small teeth at the base of the petiole, and inflorescences usually shorter than the leaves, whereas *B. calcarea* has unarmed petioles and inflorescences exceeding the length of the leaves. *Brahea berlandieri*, which is currently synonymized with *B. dulcis* (Govaerts and Dransfield, 2005; Hodel 2006; Govaerts et al., 2018; Hodel, 2018), occurs in northeastern Mexico, and was originally distinguished by having shorter rachillae than *B. dulcis* by Quero and Yáñez (2000). Though synonymized, it is unclear whether *B. berlandieri* is distinct from *B. dulcis* or whether it is a local form of the latter in northeastern Mexico. The two dwarf species *B. decumbens* (montane, limestone soils in open, rocky sites) and *B. moorei* (limestone soils in montane oak forest understory) differ in that *B. decumbens* has blue-gray leaves and a branching, creeping trunk, whereas *B. moorei* has leaves green adaxially and chalky white abaxially, is solitary, and appears trunkless. Quero (2000) subsequently described *Brahea sarukhanii* from a narrow region of Nayarit and Jalisco in central-western Mexico, but this species is of uncertain affinity in that it displays characteristics of both subgenera, including small teeth near the base of the petiole and relatively smaller fruits. Hodel (2006) distinguishes this species from the widespread and co-occurring *B. dulcis* by the persistence of old leaf bases along the entire length of the trunk as opposed to only along the upper third of the trunk (*B. dulcis*).

Despite recent taxonomic progress, there has been no explicit phylogenetic analysis of relationships in *Brahea*. Furthermore, the existence of morphological intermediacy, environmental and local variation, and hybridization/introgression (e.g. Ramirez-Rodríguez *et al.*, 2011) have likely precluded a definitive understanding of taxonomy in this genus. *Brahea* presents striking variation in growth form, with some species being trees of tall-to-medium stature at one extreme, some of variable or intermediate height (e.g. *B pimo, B. aculeata*), and some having small, acaulescent, creeping, shrub-like, or cespitose growth forms (e.g. *B. decumbens, B. moorei*). The two dwarf species, *B. decumbens* and *B. moorei*, grow in sympatry

in northeastern Mexico, calling into question whether these species are closely related, or if they represent convergent growth forms within the genus. Thus *Brahea* represents a highly appropriate system in which to test the hypothesis that height and DNA substitution rates are negatively correlated (sensu Lanfear et al., 2013).

Species of *Brahea* occupy a wide variety of environmental conditions across the geographic range of the genus, from northern Mexico to Nicaragua, where they often represent major ecosystem structural components, especially in desert and other xeric habitats (Uhl & Dransfield, 1987; Henderson *et al.*, 1995; Quero, 2000; Hodel, 2006; Dransfield, Uhl, *et al.*, 2008; Wehncke *et al.*, 2013). However, the biogeographic history of this clade is unknown, and likely complex, potentially having been shaped by vicariance, dispersal, and sympatric speciation across a geologically dynamic landscape (e.g. Sedlock *et al.*, 1993). The geological history of Mexico is also complex, with several major events having occurred over the last few tens of millions of years that could have potentially shaped distributions and species divergence in *Brahea*. These include the formation of: (1) the Mexican Transvolcanic Belt ca. 15 million years ago (mya), bisecting mainland Mexico to the north and south; (2) the opening of the Gulf of California, separating Baja California from western mainland Mexico ca. 7.2 mya; and (3) the formation of Guadalupe Island via volcanic activity also around 7.2 mya (Ferrari *et al.*, 2012; Bennett and Oskin, 2014; Dolby *et al.*, 2015). It is currently unknown if or how these processes influenced diversification and dispersal in *Brahea*.

In addition to the potential allopatric influence of geological processes in diversification, several species of *Brahea* have contemporary, overlapping ranges, and may exemplify cases of sympatric niche differentiation and speciation. For example, *B. armata* overlaps with *B. aculeata* and *B. brandegeei* in northwestern Mexico, while *B. dulcis* overlaps with *B. calcarea*, *B. pimo*, *B. moorei*, *B. sarukhanii*, *B. decumbens*, and the synonymous "*B. berlandieri*" on mainland Mexico. Species distribution models (SDMs) allow us to test for ecological scenarios potentially underlying species diversification (Nunes and Pearson, 2017). We can test for phylogenetic niche diversification vs. conservatism (Harvey and Pagel, 1991; reviewed in Pyron *et al.*, 2015) by assessing the equivalence of inferred niche space between species pairs relative to niche differences due to random chance. We expect to find closely-related species that occupy distinct niche spaces, often with overlapping ranges or in close proximity.

Here we use a combination of genome skimming (plastid and mitochondrial genomes, ribosomal DNA cistrons) and Sanger sequencing of single-copy nuclear introns to generate a phylogenomic dataset of approximately 400 kb. Our specific objectives are to: (1) provide resolution and support for species-level phylogenetic relationships within *Brahea* and to test the current subgeneric circumscription; (2) test the putative association between plant height and substitution rate in a phylogenetic context via ancestral state reconstruction; (3) infer divergence times and biogeographic history; and (4) test for niche differentiation among closely related, geographically overlapping species. This study has implications for Central American biogeography (more prominent roles for dispersal and sympatric speciation than for allopatric speciation via vicariance), patterns of ecologically driven species diversification (sympatric

niche differentiation), growth form evolution, horticulture, and conservation of these ecologically important palms.

MATERIALS AND METHODS

Phylogenetic analyses

***Taxon sampling and DNA* sequencing**. We sampled all 11 species currently recognized in *Brahea* (Table 1, including *Washingtonia robusta* and *Chamaerops humilis* as outgroups; Hodel, 2006; Govaerts et al., 2018), extracted DNAs using the CTAB method (Doyle and Doyle, 1987), and used standard procedures for Illumina library preparation and sequencing [Supplementary Information, Methods]. We amplified nuclear intron regions, corresponding to the Malate Synthase (*MS*) gene; Serine/Threonine Protein Kinase genes *CISP4* and *CISP5*; and DNA-directed RNA Polymerase Subunit Beta gene (*RPB2*) [Supplementary Information, Methods].

DNA assembly, alignment and phylogenetic analyses. We assembled plastid, mitochondrial, and rDNA contigs de novo in NOVOPlasty (version 2.6.3; Dierckxsens *et al.*, 2016), and extended contigs in GENEIOUS v.11 (Biomatters Ltd., New Zealand). We aligned plastomes in MAFFT v.1.33 (Katoh and Standley, 2013), and MUSCLE (Edgar, 2004), and removed positions containing gaps. We subjected both separate and concatenated alignments to phylogenetic analysis under Parsimony, Maximum Likelihood, Bayesian, and quartet-based methods. We conducted: Parsimony searches in TNT with 2,000 jackknife replicates (Goloboff *et al.*, 2008); Maximum Likelihood (ML) searches in RAxML v.8 under a GTRGAMMA model with 1,000 standard bootstrap replicates (Stamatakis, 2014); Bayesian analyses in MrBayes v.3.2.6 (Ronquist *et al.*, 2012) for 10^7 generations (GTR+Gamma+I model) and with the first 25% as burn-in; and quartet-based methods in SVDquartets using both concatenated and coalescent models, each with 1,000 bootstrap replicates (Chifman and Kubatko, 2014; 2015) [details of these analyses can be found in Supplementary Information, Methods]. We quantified congruence and conflict among ML topologies based on plastid, mitochondrial, nuclear rDNA, and nuclear introns using Robinson-Foulds (RF) tree distances (Robinson and Foulds, 1979) in PAUP v.4.0 (Swofford, 2002).

Growth form evolution

We reconstructed the evolution of growth form among species of *Brahea* by using maximum plant height following values in Henderson *et al.* (1995), Quero (2000), and Quero and Yáñez (2000). We used the R (R Core Development Team, 2014) packages ‘ape’ (Paradis, 2004) and ‘phytools’ (Revell, 2012) to infer ancestral values for height under a Maximum Likelihood Brownian Motion model, based on the combined, total evidence tree with branch lengths converted to ultrametric via non-parametric rate smoothing (Sanderson, 1997) in R. We computed root-to-tip GTR distances using the ‘vcv.phylo’ function on the non-smoothed phylogram from above, and regressed these on maximum height values using standard and phylogenetic regression via Independent Contrasts (Felsenstein, 1980; Garland *et al.*, 1992) in the R package ‘ape’. We tested for phylogenetic signal in both maximum height and GTR-based branch lengths from the combined RAxML tree using Pagel’s λ.

Biogeographic analyses

Divergence time estimation. We estimated divergence times among species of *Brahea* in BEAST2 (Bouckaert *et al.*, 2014) under a Lognormal Relaxed Clock (Drummond *et al.*, 2006) and a GTR+Gamma+I substitution model with parameters estimated from the data. We added data from all *Brahea* species to the dataset of Couvreur *et al.* (2011), for a total of nine loci [see Supplementary Information, Methods for additional details]. We chose four calibration points with exponential priors, to be consistent with the analysis of Couvreur *et al.* (2011): *Sabalites* (Berry, 1914), to calibrate the stem node of Coryphoideae at [minimum age offset = 85.8 million years ago (mya), mean = 1.0]; *Mauritiidites* (Schrank, 1994) to calibrate Mauritiinae (minimum age offset = 65.0 mya, mean = 1.5); a *Cocos*-like fossil to calibrate subtribe Attaleinae (minimum age offset = 54.8 mya, mean = 2.0); and *Hyphaenae kapelmanii* (Pan et al., 2006) to calibrate the stem node of Hyphaeninae (minimum age offset = 27.0 mya, mean = 0.5). We also constrained the stem node of palms (i.e. palms + Dasypogonaceae) to have arisen between 110-120 mya (these dates were used as the 95% prior on a normal distribution with a mean of 115 mya). We ran BEAST2 for 2×10^8 generations of the MCMC, sampling every 5×10^4 generations, discarding the first 30% of samples as burn-in after a pre-burn-in period of 10^5 samples. We verified stationarity via effective samples sizes >200 for each parameter in TRACER (Rambaut *et al.*, 2014), and also verified convergence of parameter values by combining results of three independent runs of BEAST2 from random starting seeds.

Ancestral range reconstruction. We used the chronogram from BEAST2 to infer ancestral ranges of *Brahea* species in BioGeoBEARS (Matzke, 2014). We chose six areas, corresponding to major physiographic regions of Mexico and Central America (e.g. Thayer, 1916; Riddle *et al.*, 2000; Bennett and Oskin, 2014): A) the Baja Californian Peninsula; B) northwestern mainland Mexico, containing the Sierra Madre Occidental, Sonoran Basin-and-Range, and Pacific Coastal Plain; C) northeastern Mexico, containing the Sierra Madre Occidental, the Great Plain, and the Northern Gulf Coast Plain; D) central/southern Mexico, containing the Mexican Transvolcanic Belt and the Southern Sierra Madre; E) southeastern Mexico and Central America; and F) Guadalupe Island. We used a time-stratified approach, with two time intervals (25.7-7.2 mya, and 7.199-0 mya), corresponding to the formation of Guadalupe Island and the Gulf of California (i.e. the separation of Baja California from mainland Mexico) approximately 7.2 million years ago (Bennett and Oskin, 2014). We used no constraints between directly adjacent areas (i.e. dispersal probabilities of 1.0), a dispersal probability of 0.5 for non-adjacent areas, and a probability of 0.1 for dispersal probability between Baja California and southeastern Mexico/Central America. For the first interval (25.7-7.2 mya), dispersal probability between Guadalupe Island and all other areas was set to zero, and then to 0.01 for the second interval (7.199-0 mya). Also in the second interval, we set dispersal probability at 0.1 between Baja California and northwestern mainland Mexico. We used the BayAreaLike+j model in BioGeoBEARS (Matzke *et al.*, 2014).

Species distribution modeling and ecological niche differentiation. We inferred species distribution models (SDM) to: (1) determine if the contemporary ranges of *Brahea* species can be modeled using available bioclimatic predictor variables; (2) test signal of niche divergence for selected pairs of *Brahea* species with overlapping ranges; (3) assess the degree to which SDMs can inform taxonomic boundaries in the group. We obtained occurrence data for all species included in this study via the Global Biodiversity Information Facility (GBIF.org, accessed 16 January 2018), followed by filtering both manually and using the 'trim.occ' R function of Nunes and Pearson (2017).

We produced SDMs using MaxEnt (version 3.4.1; Phillips *et al.*, 2017) through the R package Dismo (version 1.1-4; Hijmans *et al.*, 2017). Two environmental datasets were used for SDMs: the entire WorldClim dataset (version 2.0; Fick and Hijmans, 2017), and a Pearson correlation-filtered version, both at ten-minute resolution [see Supplementary Information, Methods for additional details]. We tested pairs of species in the *B. armata* clade, and between "*B. berlandieri"* and *B. dulcis* for niche equivalency (Warren *et al.*, 2008) and phylogenetic niche conservatism (Harvey and Pagel, 1991; see Pyron *et al.*, 2015). We used the R function 'nicheEquivalency' in the Dismo package to conduct Warren's Identity test; and the 'Random Translocation and Rotation' (RTR) and the modified niche overlap (MO) metric of Nunes and Pearson (2017) to test for Phylogenetic Niche Conservatism (RTR and MO are hereafter collectively referred to as the RTR-MO). We adjusted our alpha level for comparisons made of species in the *B. armata* clade using Bonferroni correction ($\alpha_{adjusted} = 0.016$).

RESULTS

Datasets. Features of all molecular datasets included in this study are summarized in Table 2. The complete plastome alignment of 11 *Brahea* and two outgroup taxa (*Chamaerops*, *Washingtonia*) is 132,870 bp in length. Removal of all sites with gaps/missing data and ambiguity codes produced an alignment of 121,301 bp with 333 parsimony-informative sites. Four contiguous regions of the mitochondrial genome were included here (approximately 67, 91, 52, and 25 kb, respectively), totaling 261,650 bp when concatenated. After removing gaps and ambiguities as above, the total aligned length was 212,874 bp with 304 Parsimony-informative sites. Amplicons for *CISP5* showed clear evidence of double banding, and so this locus was excluded from further analysis. The total, combined dataset was 342,142 bp in length, with 756 PIC. Data are deposited under GenBank accession numbers XXXXXX-XXXXXX.

Phylogenetic analyses

Plastomes. Parsimony, Maximum Likelihood, and Bayesian analyses of whole aligned plastomes, with one copy of the IR removed, yield highly resolved and strongly supported relationships [Fig. 1A; Supplementary Information, Fig. S1]. *Brahea* is supported as monophyletic (Parsimony Jackknife = 100, ML Bootstrap = 100, Bayesian Posterior Probability = 1.0; denoted as '100, 100, 1.0' hereafter), within which there are two strongly supported principal clades. The first of these (100, 100, 1.0) contains *B. decumbens*, *B. calcarea*, *B. dulcis*, and *B. berlanderi* (hereafter referred to as the '*B. dulcis* clade'). The latter two accessions share a close relationship (89, 94, 1.0), but relationships among *B. decumbens*, *B. calcarea*, and the clade of (*B. berlanderi*, *B. dulcis*) are unresolved. The next clade contains all remaining *Brahea* (100, 98, 1.0), and is further divided into two clades within which all relationships are strongly supported (≥97, 1.0). The dwarf species *Brahea moorei* is sister to *B. sarukhanii* (100, 100, 1.0), while *B. pimo* is sister to *B. salvadorensis* (100, 100, 1.0), and these two clades are sister to one another (100, 100, 1.0; hereafter referred to as the *B. pimo* clade). Sister to this is a clade composed of (*B. armata*, *B. aculeata*; 90, 93, 1.0), successively sister to *B. brandegeei* (98, 97, 1.0), and *B. edulis* (100, 100, 1.0), hereafter referred to as the '*B. armata* clade.'

Mitochondrial DNA. Relationships overall are less strongly supported for mtDNA than for plastomes (Fig. 1B). The three primary clades recovered from the plastome data are also recovered for mtDNA. A notable difference is the placement of the *B. dulcis* clade as sister to the *B. pimo* clade, collectively sister to the *B. armata* clade, but this relationship is weakly supported (54, 78, 0.99). Many sister relationships are identical to those from the plastome and are well supported (e.g. *aculeata+armata; moorei+sarukhanii; pimo+salvadorensis*), while remaining sister relationships among species that differ from those of the plastome receive weak support.

Nuclear DNA. Relationships based on nuclear ribosomal DNA (rDNA) are highly identical to those based on plastomes, albeit with lower support overall, and differing only in the placement of *B. decumbens* [Supplementary Information, Fig. S1]. Both Malate Synthase (*MS*) and *CISP4* recover the same 'deep' tree structure among the three principal clades, but with

weak support individually [Supplementary Information, Fig. S1]. *RPB2* displays several relationships not observed for any other locus, but most have weak support; e.g., *B. moorei* and *B. brandegeei* group in a clade of *B. dulcis*, *B. berlandieri*, and *B. calcarea* [Supplementary Information, Fig. S1].

Combined analyses. Combined nuclear data (rDNA, *MS*, *CISP4*, and *RPB2*) yield a highly supported topology similar to that based on plastomes, differing only in the placement of *B. decumbens* (Fig. 1C). Analysis of the concatenated dataset from all three genomes recovers a highly supported tree (Fig. 1D; all support values >94). These relationships differ from those of the plastome only in the placement of *B. decumbens* as sister to (*B. calcarea*, (*B. dulcis*, *B. berlandieri*)). Analysis in SVDquartets (specifying one tree for all sites) yields an identical topology to those based on Parsimony, Maximum Likelihood, and Bayesian Analysis [Supplementary Information, Fig. S2]. In this SVDquartets analysis, a topology of (*B. edulis*, (*B. brandegeei*, (*B. armata*, *B. aculeata*))) is recovered with 100% Bootstrap support for all relationships; by contrast, a topology of (*B. brandegeei*, (*B. edulis*, (*B. armata*, *B. aculeata*))) is recovered under the multispecies coalescent model, with only 39% Bootstrap support for the placement of *B. edulis* as sister to (*B. armata*, *B. aculeata*). A second coalescent-model analysis in SVDquartets, specifying the 'Erik+2' parameter, places *B. edulis* as sister to *B. brandegeei* with low support (Bootstrap = 54), and these are sister to (*B. armata*, *B. aculeata*). Thus, there is little support in coalescent analyses for the relative placement of *B. edulis* and *B. brandegeei* within the *B. armata* clade.

Robinson-Foulds tree distances on average were greatest between the *CISP4* topology and all other topologies [Supplementary Information, Table S1]. Out of the three largest single-genome alignments (i.e. combined nrDNA, mtDNA, and plastomes), the combined nuclear tree had the lowest RF distance to the total combined tree (2×RF = 0), followed by the plastome tree (2×RF = 2), and the mtDNA tree (2×RF = 6).

Growth form evolution

Maximum height in *Brahea* ranges from 0.4 m in *B. moorei* to 15 m in *B. armata*. The tallest species occupy the *B. armata* clade [ancestral value = 10.63 ± 2.08 m (i.e. ± one standard deviation)], while the shortest species occupy the *B. pimo* clade (ancestral value = 5.32 ± 2.31 m) (Fig. 4). Both of these clades comprise subgenus *Erythea* sensu Quero and Yáñez (2000) (ancestral value = 6.95 ± 2.63 m). The ancestor of subgenus *Brahea* is estimated to have had a maximum height of 6.37 ± 1.85 m. Maximum height shows a strong relationship with root-to-tip branch lengths, which range from 0.000469 substitutions·site^{-1} (s·s^{-1}) in *B. dulcis* to 0.000803 s·s^{-1} in *B. moorei* ($F = 32.94$, df =11, $p = 0.00013$). However, this relationship is non-significant when correcting for phylogenetic relationships via Independent Contrasts ($F_{pic} = 0.002$, df = 10, $p = 0.96$), suggesting that any relationship between these traits is better explained by shared ancestry. Pagel's λ, a measure of phylogenetic signal, was significantly different than a model of λ = 0 for root-to-tip branch lengths (λ = 1.06, P = 0.0009), but not for maximum height (λ = 0.61, P = 0.15). The two shortest species likely evolved from taller ancestors: maximum height in *B.*

decumbens is 2.5 m vs. the ancestral value of 6.37 ± 1.85 m for the *B. dulcis* clade, while in *B. moorei* maximum height is 0.4 m vs. the ancestral values of 5.14 ± 2.17 m for (*B. moorei, B. sarukhanii*).

Biogeographic analyses

Divergence time estimation. The estimated stem-node age of *Brahea* is 25.6 million years ago (mya), with a 95% highest posterior density (HPD) of 14.8-35.5 mya, while the crown age of *Brahea* is estimated to be 15.6 mya (9.1-22.2) (Fig. 2). Estimates of the crown radiations of the three principal clades of *Brahea* are: 5.5 mya (2.1-9.8) for the *B. armata* clade; 7.6 mya (3.3-12.0) for the *B. pimo* clade; and 6.2 mya (2.2-11.1) for the *B. dulcis* clade. *Brahea armata* and *B. aculeata* likely diverged relatively recently (1.36 mya, 0.05-2.6), as did *B. dulcis* and *B. berlandieri* (0.5, 0.00-1.4).

Ancestral range reconstruction. We inferred an ancestral range of AB for the *B. armata* clade (Fig. 3; Baja California + northwestern mainland Mexico), and all nodes within this clade are estimated to share the same ancestral range, all with high likelihood percentages for the BayAreaLike+j model ($L_{\%} > 0.95$). However, $L_{\%}$ is substantially lower when the 'j' parameter is excluded. *Brahea edulis* shows a high $L_{\%}$ of having arisen via founder event speciation on Guadalupe Island when including the 'j' parameter (jump dispersal). Ancestral ranges are more ambiguous in the *B. pimo* clade (Fig. 3), with estimates of C (northeastern Mexico) or D (central/southern Mexico) for the ancestral ranges of *B. moorei* and *B. sarukhanii*, and D or E (southeastern Mexico/Central America) as the ancestral range of *B. pimo* and *B. salvadorensis*. An ancestral range of BDE or BCDE (northwestern mainland Mexico, central/southern Mexico, southeastern Mexico/Central America) is inferred for the common ancestor of the *B. dulcis* clade ($L_{\%} = 0.60$ including 'j'; $L_{\%} = 0.10$ excluding 'j'). The ancestral range of *Brahea* as a genus is equivocal based on the current analysis (BDE $L_{\%} = 0.18$ including the 'j' parameter; ABCD $L_{\%} = 0.04$ excluding 'j').

Species distribution modeling and ecological niche differentiation. We rejected equivalency of SDMs for all comparisons between species pairs of interest (Table 3). RTR-MO tests identified signal of niche divergence between *B. brandegeei* and *B. aculeata* (P = 0.00983, Supplementary Information, Fig. S3], as well as between *B. aculeata* and *B. armata* [P = 0.00031, Supplementary Information, Fig. S3). Niche space overlap between *B. brandegeei* and *armata* falls below the established 5% CI of the null distribution, but is not significantly different from the null post-Bonferroni correction (P = 0.0374; $\alpha_{adjusted}$ critical value = 0.016). The RTR-MO test also failed to reject that the observed overlap between *B. berlandieri* and *dulcis* significantly differed from the null distribution (P = 0.216).

We ultimately excluded approximately half of the GBIF localities, after manually and ecologically filtering outliers resulting from: taxonomic uncertainty, obvious cultivation out of the native range, or a lack of georeferencing/coordinate certainty [Supplementary Information, Table S2]. We identified no major differences between published species ranges and the extents of our filtered localities or replicated SDMs, with the exceptions of *B. calcarea* and *B. decumbens*, based on visual cross-validation using range maps of Henderson *et al.* (1995).

Analyses using our Pearson-filtered predictor dataset conservatively resulted in more overestimation of SDM extent, relative to those using the entire Worldclim dataset. The SDMs and associated downstream tests we report were based on the Pearson-filtered dataset [Supplementary Information, Table S2], in order to minimize false positives (which can be attributed to uncertainties associated with the use of publicly available data), and model overfitting.

MaxEnt analyses accurately predict the present-day extent of *Brahea* species using Bioclim variables [Supplementary Information, Table S3]. Models did not appreciably vary between MaxEnt replicates, and the predictor variables that contributed the most to each SDM were found to be both suitable and stable, as judged by marginal and SDM-specific response curves [see Supplementary Information, Link 1]. Area under the curve of the receiver operator characteristic, and the percent contributions of predictor variables to each SDM is reported in Supplementary Information, Table S4. The majority of variation observed between SDM extents was attributable to over-prediction of areas of low occurrence probability (< 0.4). Unique combinations of environmental predictor variables influenced the SDM of each species [Supplementary Information, Table S4], but some clade-specific predictor variable influences are evident. Over-prediction of occurrence and coarser resolution of predictor variables here result in more conservative results (though this may seem counterintuitive), since each measures observed overlap of estimated niche space. The extent of SDMs for *B. nitida* and *B. decumbens* were strongly over-predicted relative to published ranges, including many points outside of the predicted range, and a small area of occurrence, respectively. We thus chose not to include these two species in tests of niche equivalency or phylogenetic niche conservatism in the *B. dulcis* clade, considering the perceived low quality of SDMs inferred for *B. nitida* and *B. decumbens*.

DISCUSSION

Palm systematics has been a challenge due to a combination of morphological homoplasy and extremely slow plastid DNA substitution rates (Uhl and Dransfield, 1987; Uhl *et al.*, 1995; Gaut *et al.*, 1992; Barrett *et al.*, 2016a). Because of this, palm systematists have turned to genome-scale datasets, as these greatly increase the number of informative characters available for phylogenetic analyses (Barrett *et al.*, 2016a; Comer *et al.*, 2015; 2016; Barrett *et al.*, 2016b; Heyduk et al, 2016). Here we have sequenced over 400 kb of DNA from all three plant genomes, largely resolving and providing support for relationships among currently known species of *Brahea*. Furthermore, this study is the first to estimate divergence times, ancestral ranges, ancestral growth forms, and ecological niche space for this highly variable, taxonomically complex, and ecologically/economically important (e.g. Pulido and Coronel-Ortega, 2015) group of American palms.

Phylogenetic Analyses

Despite the large amount of data generated per species of *Brahea*, we recovered fewer than 1,000 total informative positions from three genomes for our combined analysis. Yet, this number was sufficient to provide highly supported relationships among species of *Brahea*. Information content varies from an average of 1.2 informative sites/1,000 bp in mtDNA to 33.1 sites/1,000 bp in nuclear *CISP4* (Table 2), underscoring the importance and power of including nuclear DNA in phylogenetic analyses of palms (e.g. Heyduk *et al.*, 2016).

Concatenated analyses yield high support for a single set of relationships, but coalescent based analyses in SVDquartets differ in the placement of *B. edulis/B. brandegeei* of the *B. armata* clade, with little to no support [Fig. 1; Supplementary information, Fig. S1 and S2]. Differing relationships based on coalescent methods indicate potential conflict among datasets, suggesting that incomplete lineage sorting, gene flow, or both may influence the recovered relationships in *Brahea*. This finding underscores the need to include many nuclear loci and multiple representatives of each putative species, such that scenarios of ILS and gene flow can be modeled and explicitly differentiated. Ways to accomplish this include examining the distribution of gene trees via concordance factors (e.g. Ané, 2007; Crowl *et al.*, 2017), or using methods that specifically incorporate gene flow (e.g. Jackson *et al.*, 2017; Morales *et al.*, 2017).

The two principal clades recovered here correspond closely to the subgenera *Brahea* and *Erythea* recognized by Moore (1973), Uhl and Dransfield (1987), Quero and Yáñez (2000), and Hodel (2006). *Brahea moorei*, a dwarf species from northeastern Mexico, is strongly supported as being a member of subgenus *Erythea*, in contrast to its placement in subgenus *Brahea* by Quero and Yáñez (2000). The more recently described *Brahea sarukhanii* (Quero, 2000), hitherto unplaced among other species of *Brahea*, shows a highly supported sister relationship to *B. moorei*, despite its caulescent habit and restricted distribution in Jalisco/Nayarit of western central Mexico.

Only two other studies to date have included multiple representatives of *Brahea*. Bacon *et al*. (2012) addressed biogeographic questions in the diverse fan palm tribe Trachycarpeae, which includes *Brahea*. Their analysis included four species of *Brahea*; three accessions of *B. dulcis* were sister to a clade of (*B. aculeata*, (*B. armata*, *B. brandegeei*)). Though sampling is limited in that study for *Brahea*, there is some agreement with the current study in that *B. dulcis* is separated from the *B. armata* clade. In that study, *B. brandegeei* is sister to *B. armata*, as opposed to *B. aculeata* being sister to *B. armata* in the current study, though this relationship is only moderately supported in the former. Klimova *et al.* (2017) used population-level sampling to address biogeographic questions in *Washingtonia robusta, W. filifera, Brahea armata, B. brandegeei*, and *B. edulis* in Baja California and Guadalupe Island; they also included a single specimen identified by the authors as '*B. elegans*' (synonymized with *B. armata*) from eastern Sonora. Sequencing over 2 kb of plastid DNA yielded no variation among *B. armata*, *B. brandegeei*, and *B. edulis*, but their sample identified as *B. elegans* differed by five plastid substitutions, suggesting this sample might be more closely allied with another species of *Brahea* (Klimova *et al.*, 2017). Nuclear DNA sequencing yielded evidence of haplotype sharing among *B. armata*, *B. brandegeei*, and *B. elegans*, but a distinct haplotype for *B. edulis* from Guadalupe Island. Their findings further suggest a complex evolutionary history of *Brahea* in the region, and highlight the possibility of gene flow within the *B. armata* complex, though this cannot be distinguished from incomplete lineage sorting based on their data. Future sampling efforts should include numerous high-variation nuclear markers, complete or nearly complete organellar genomes, and a comprehensive sampling of multiple individuals from all currently recognized species of *Brahea* across their respective geographic ranges.

Growth form evolution

Maximum Likelihood reconstruction of plant height suggests that the ancestor of *Brahea* was a medium-statured tree (6.85 ± 3.04 m). Estimated ancestral heights change little moving from the root ancestor in Fig. 4 to the ancestors of the *B. pimo* and *B. dulcis* clades, but increase dramatically in the ancestor of the *B. armata* clade, which contains all of the tallest species of *Brahea*. Interestingly, the two shortest species, *B. moorei* and *B. decumbens*, each likely evolved from medium-statured, caulescent ancestors, from which they diverged ca. 5.1 and 6.2 mya, respectively. The latter findings are likely responsible for the non-significance of phylogenetic signal in maximum plant height based on Pagel's λ. Dwarf or small-statured palm species are often closely related to medium or tall-statured species (e.g. the dwarf species *Sabal minor* and *S. etonia*; Zona, 1990; Henderson *et al.*, 1995; Heyduk *et al.*, 2016), suggesting evolution in height differences can be rapid, as is the case between *B. moorei* and *B. sarukhanii*, and *B. decumbens* and taller members of the *B. dulcis* clade. *Brahea moorei* and *B. decumbens* are often referred to as dwarf species, yet they differ in some key ways. First, *B. moorei* has a short, solitary, rhizomatous, subterranean trunk (more rarely, the trunk can be aboveground), giving the plant a low-growing, shrub-like appearance (Henderson *et al.*, 1995; Hodel, 2006). *Brahea decumbens*, on the other hand, has a short, clustered, above-ground trunk, and often assumes a creeping habit

(hence the species name '*decumbens*'), but is sometimes erect. In fact, as Hodel (2006) observed, there are many intermediate forms between *B. decumbens* and the widespread *B. dulcis*, suggesting environmental or local variation, and quite possibly gene flow among these species.

A recent study across flowering plants demonstrated a large-scale relationship between plant height and substitution rates, when controlling for other factors such as species richness and latitude (Lanfear *et al.*, 2013), in which taller plants tend to have slower rates of substitution. This situation is pronounced in palms, which display some of the lowest substitution rates among monocots, and are unequivocally the tallest of the monocots (Barrett *et al.*, 2016a). Here, although these patterns exist at broad taxonomic scales (e.g. across angiosperm orders and families), it is unknown whether they also exist at finer taxonomic scales. Thus, we used *Brahea* as a case to address whether this pattern holds at finer taxonomic levels. Though there is an apparent negative correlation between substitution rate and height, this relationship is better explained by common ancestry, as indicated by Phylogenetically Independent Contrasts and significant phylogenetic signal in branch lengths based on Pagel's λ. The relationship between substitution rates and height in plants has been explained by the 'rate of mitosis' hypothesis (Lanfear *et al.*, 2013), in which taller plants typically experience a slow-down of mitosis as they reach maximum height, and thus fewer potential mutations are passed on via reproductive tissues relative to the situation in shorter species. However, both *B. moorei* and *B. decumbens*, the two shortest *Brahea* species, are also extremely slow-growing (Hodel, 2006; S. Lahmeyer, personal observation), which may obscure any potential effect of plant height on heritable substitution rates in the genus, if such a relationship exists. Alternatively, the relationship may not exist at such low taxonomic levels, in which tall vs. short forms have recently evolved, and differences in substitution rates may potentially be determined by a number of factors differing on a taxon-by-taxon basis, as suggested by Barrett *et al.* (2016a).

Biogeographic analyses

Divergence time estimates and ancestral range reconstruction. The stem and crown age estimates of *Brahea* (approximately 25.7 and 15.6 mya, respectively; Fig. 2) correspond closely with those in a previous study that included some accessions of *Brahea* (Bacon *et al.*, 2012). Our estimates suggest that ancestral forms of *Brahea* were present during some of the major geological events in Mexico, including the formation of the Transvolcanic Belt in Central Mexico (starting in the mid-Miocene, ca. 15 mya; Ferrari *et al.*, 2012), the Gulf of California (ca. 7.2 mya; Bennett and Oskin, 2014), and Guadalupe Island (also 7.2 mya), all around the same time (Dolby *et al.*, 2105).

The earliest divergence in *Brahea* corresponds approximately with the onset of formation of the Transvolcanic Belt in Mexico ca. 15 mya, though the estimated ancestral range of the common ancestor of all *Brahea* is equivocal based on our analysis in BioGeoBears (Fig. 3). Thus it is unclear if this geological process may have influenced diversification in *Brahea*. The most likely ancestral range for subgenus *Erythea* is Baja California and northwestern Mexico, but with low confidence. Even so, it is clear that geography has played a role in diversification in *Brahea*,

with the *B. armata* clade concentrated in the northwest, members of the *B. pimo* clade occupying central, northeastern, and southeastern Mexico/Central America, and the *B. dulcis* clade occupying all areas but Baja California and Guadalupe Island.

The radiation of the *B. armata* clade began an estimated 5.51 mya (HPD = 2.13-9.84), which overlaps with the formation of Guadalupe Island and the Gulf of California (Bennett and Oskin, 2014). Jump dispersal (i.e. founder event speciation) can be attributed to the origin of *B. edulis* on Guadalupe Island. Based on Fig. 3, it is likely that the ancestor of *B. edulis* colonized Guadalupe Island soon after its formation (ca. 7.2 mya), and has since existed in isolation. The exact position of *B. edulis* varies among analyses here, either as sister to the remaining members of the *B. armata* clade, or as sister to (*B. armata*, *B. aculeata*) (Figs. 2, 3). Thus, it is unknown whether dispersal of the ancestral form of the *B. armata* clade occurred before or after the evolution of *B. brandegeei* in Baja California.

The ancestral range for the *B. armata* clade (Baja California and Northwestern Mexico) suggests the following sequence of biogeographic events were possible based on interpretation of Fig. 3: (1) sympatric range-copying in the ancestor of *B. brandegeei* and the remaining members of the *B. armata* clade; (2) founder event speciation as a result of jump dispersal of the ancestor of *B. edulis* to Guadalupe Island; and (3) subset/sympatric speciation of *B. aculeata* (northwestern Mexico) and *B. armata* (Baja California and northwestern Mexico). These findings contrast with those in other studies suggesting that the formation of the Gulf of California represents a major driver of allopatric speciation via vicariance (e.g. Riddle *et al.*, 2000). Instead, most speciation events in this clade likely occurred after the separation of Baja California from western mainland Mexico, suggesting roles for sympatric speciation or dispersal, especially in the case of *B. edulis*.

It is more difficult to interpret the estimated biogeographic history of the *B. pimo* clade, due to the equivocal likelihood percentage of its ancestral range in both models (Fig. 3). However, all speciation events in this clade potentially overlap with the ongoing formation of the Transvolcanic Belt in central Mexico, and thus it is unknown whether the later stages of volcanic uplift would have contributed to, for example, the divergence of *B. moorei* in northeastern Mexico and *B. sarukhanii* in central/western Mexico. Our results suggest a larger role for dispersal to neighboring areas than for vicariance and allopatric speciation due the formation of the Transvolcanic Belt (Fig. 3).

DEC-like models, and especially those carrying the 'j' parameter have been criticized recently, in that they fail to properly model cladogenetic events by preferentially biasing analyses towards cladogenesis (as opposed to anagenetic processes), and artificially inflating conclusions of jump dispersal/founder event speciation (Ree and Sanmartín, 2018). Therefore, we interpret our findings cautiously, and conclude that our proposed ancestral ranges for the species of *Brahea* are largely equivocal. The biogeographic history of Mexico and Central America is complex, and our ability to reconstruct the history of *Brahea* is limited in this case. Additional sampling within species, improved taxonomic delimitations, and more appropriate models including anagenetic and cladogenetic change in a time-dependent fashion while incorporating

584 phylogenetic uncertainty (e.g. ClaSSE-type models; Fitzjohn, 2012) may help improve estimates
585 of ancestral ranges in *Brahea*.
586 ***Species distribution models and ecological niche differentiation.*** Here we tested for
587 signal of ecological diversification among selected species pairs within the *B. armata* and *B.*
588 *dulcis* clades. These clades contain the youngest nodes in our chronogram, display overlapping
589 species ranges in some cases, and contain taxonomic boundaries that remain somewhat uncertain
590 (e.g. in the *B. dulcis* clade). The recent origin of *Brahea aculeata* and *armata* may be the result
591 of sympatric ecological diversification in novel habitats. The respective SDMs of *Brahea*
592 *aculeata* and *armata* are unique, even though their geographic ranges overlap. *Brahea*
593 *brandegeei* and *armata* are distributed in Baja California and northwestern mainland Mexico,
594 while *B. aculeata* is found only in northwestern mainland Mexico (Henderson *et al.*, 1995;
595 Hodel, 2006). However, filtered GBIF records did not include *B. brandegeei* localities from
596 northwestern mainland Mexico, an area listed by Henderson *et al.* (1995) to be part of this
597 species' range. Our inferences of SDMs and phylogenetic relationships between these three
598 species suggest that the northern range and possibly the taller height of *B. armata*, and an eastern
599 range extent and preference for more upland habitats by *B. aculeata*, may be evidence of
600 relatively recent niche divergence. These results provide an additional line of evidence
601 supporting our findings of sympatric speciation in the diversification of the *B. armata* clade in
602 northwestern Mexico.
603 Recent taxonomic treatments place *B. "berlandieri"* as a synonym of the widespread and
604 variable *B. dulcis* (e.g. Henderson et al., 1995; Hodel, 2006). Our inferred SDMs provide some
605 evidence for the recognition of northeastern populations of *B. dulcis* corresponding to *B.*
606 *berlandieri* (currently known as the former) as a distinct entity, raising the possibility that *B.*
607 *berlandieri* could in fact be a separate species. Despite their estimated recent divergence time,
608 their respective SDMs are significantly non-equivalent (0.18, $P = 7.09 \times 10^{-64}$). However, the
609 failure to distinguish this difference from a null distribution argues against niche divergence as
610 the force underlying any potential difference among these entities. These results coincide well
611 with an earlier caveat provided by Warren *et al.* (2014), that SDM non-equivalency is not always
612 indicative of ecological speciation, and that is likely over-prescribed in the literature. Regardless,
613 the putative distinctness of *B. berlandieri* warrants further investigation genetically,
614 morphologically, and ecologically.
615 A greater number of high-resolution, georeferenced, taxonomically-vetted specimen
616 records from across species ranges would allow us to infer higher quality estimates of occupied
617 niche space. Reducing the assumed georeferencing and taxonomic errors in publically available
618 locality datasets would allow use of higher resolution predictor variables, for which many more
619 datasets exist, e.g. Harmonized Soils, which may prove to be important in *Brahea*, given the
620 preference of some species for calcareous soils. These improved models would allow us to
621 include more *Brahea* species, such as *B. calcarea* and *decumbens*, and furthermore to extend
622 these analyses back in time to ancestral nodes.
623

CONCLUSIONS

We have conducted an explicit phylogenetic study of one of the most poorly understood, yet ecologically important groups of American palms, providing strong resolution and support for phylogenetic relationships in the genus, based on nearly 400 kb of sequence data from all three genomes. We further provide a phylogenetic test of subgeneric species assignments, largely corroborating earlier work based on diagnostic morphological characters. The exception is *B. moorei*, which is strongly supported as being a member of subgenus *Erythea*, but was previously placed in subgenus *Brahea* based on morphological characters including a lack of petiolar spines. We demonstrate the evolution of dwarf forms from taller, tree-like ancestors in *B. moorei* and *B. decumbens*. We provide the first comprehensive estimates of the timing of speciation events across the genus, reveal roles for sympatric speciation and dispersal in the biogeographic history of *Brahea*, and provide evidence of ecological niche divergence among closely related species in the *B. armata* and *B. dulcis* species complexes. The findings are relevant in elucidating complex patterns of biogeographic history in Central America and Mexico. Most importantly, we provide a framework for future studies to be conducted including integrative species delimitation within the genus, estimation of gene flow, phylogeographic history, and more fine-scale investigation of environmental/ecological factors driving evolution in this clade.

644 LITERATURE CITED
645
646 **Ané C, Larget B, Baum DA, Smith SD, Rokas A. 2007.** Bayesian estimation of concordance
647 among gene trees. *Molecular Biology and Evolution* **24**: 412-426.
648 **Asmussen CB, Dransfield J, Deickmann V, Barfod AS, Pintaud JC, Baker WJ. 2006.** A new
649 subfamily classification of the palm family (Arecaceae): evidence from plastid DNA
650 phylogeny. *Botanical Journal of the Linnean Society* **151**: 15-38.
651 **Bacon CD, Baker WJ, Simmons MP. 2012.** Miocene dispersal drives island radiations in the
652 palm tribe Trachycarpeae (Arecaceae). *Systematic Biology* **61**: 426-442.
653 **Bacon, CD, Roncal J, Andermann T, *et al.* In review.** Parallel divergence with gene flow in
654 Amazonia. *Molecular Ecology*.
655 **Baker WJ, Dransfield J. 2016.** Beyond Genera Palmarum: progress and prospects in palm
656 systematics. *Botanical Journal of the Linnean Society* **182**: 207-233.
657 **Baker WJ, Savolainen V, Asmussen-Lange CB, *et al*. 2009.** Complete generic-level
658 phylogenetic analyses of palms (Arecaceae) with comparisons of supertree and
659 supermatrix approaches. *Systematic Biology* **58**: 240-256.
660 **Balslev H, Bernal R, Fay MF. 2016.** Palms - emblems of tropical forests. *Botanical Journal of*
661 *the Linnean Society* **182**: 195-200.
662 **Barrett CF, Baker WJ, Comer JR, *et al.* 2016a.** Plastid genomes reveal support for deep
663 phylogenetic relationships and extensive rate variation among palms and other
664 commelinid monocots. *New Phytologist* **209**: 855-870.
665 **Barrett CF, Bacon CD, Antonelli A, Cano A, Hofmann T. 2016b.** An introduction to plant
666 phylogenomics with a focus on palms. *Botanical Journal of the Linnean Society* **182**:
667 234-255.
668 **Bennett SEK, Oskin ME. 2014.** Oblique rifting ruptures continents: Example from the Gulf of
669 California shear zone. *Geology* **42**: 215-218.
670 **Berry EW.** 1914. The Upper Cretaceous and Eocene floras of South Carolina and Georgia. *US*
671 *Geological Survey Professional Papers* **84**: 1-200.
672 **Bouckaert R, Heled J, Kuhnert D, *et al*. 2014.** BEAST 2: A software platform for Bayesian
673 evolutionary analysis. *Plos Computational Biology* **10**: e1003537.
674 **Chifman J, Kubatko L. 2014.** Quartet inference from SNP data under the Coalescent Model.
675 *Bioinformatics* **30**: 3317-3324.
676 **Chifman J, Kubatko L. 2015.** Identifiability of the unrooted species tree topology under the
677 coalescent model with time-reversible substitution processes, site-specific rate variation,
678 and invariable sites. *Journal of Theoretical Biology* **374**: 35-47.
679 **Comer JR, Zomlefer WB, Barrett CF, *et al.* 2015.** Resolving relationships within the palm
680 subfamily Arecoideae (Arecaceae) using plastid sequences derived from next-generation
681 sequencing. *American Journal of Botany* **102**: 888-899.
682 **Comer JR, Zomlefer WB, Barrett CF, Stevenson DW, Heyduk K, Leebens-Mack JH. 2016.**
683 Nuclear phylogenomics of the palm subfamily Arecoideae (Arecaceae). *Molecular*

Phylogenetics and Evolution **97**: 32-42.

Couvreur TLP, Forest F, Baker WJ. 2011. Origin and global diversification patterns of tropical rain forests: inferences from a complete genus-level phylogeny of palms. *BMC Biology* **9**: 44.

Crowl AA, Myers C, Cellinese N. 2017. Embracing discordance: Phylogenomic analyses provide evidence for allopolyploidy leading to cryptic diversity in a Mediterranean *Campanula* (Campanulaceae) clade. *Evolution* **71**: 913-922.

Dierckxsens N, Mardulyn P, Smits G. 2017. NOVOPlasty: de novo assembly of organelle genomes from whole genome data. *Nucleic Acids Research* **45**: e18.

Dolby GA, Bennett SEK, Lira-Noriega A, Wilder BT, Munguia-Vega A. 2015. Assessing the geological and climatic forcing of biodiversity and evolution surrounding the Gulf of California. *Journal of the Southwest* **57**: 391-455.

Drummond AJ, Ho SYW, Phillips MJ, Rambaut A. 2006. Relaxed phylogenetics and dating with confidence. *PLoS Biology* **4**: e88.

Doyle JJ, Doyle JL. 1987. A rapid DNA isolation procedure for small quantities of fresh leaf tissue. *Phytochemical Bulletin* **19**: 11-15.

Dransfield J, Uhl NW, Asmussen CB, Baker WJ, Harley MM, Lewis CE. 2008. Genera Palmarum: the evolution and classification of palms. Kew, UK: Kew Publishing.

Edgar RC. 2004. MUSCLE: multiple sequence alignment with high accuracy and high throughput. *Nucleic Acids Research* **32**: 1792-1797.

Endlicher S. 1837. Genera Plantarum **1**: 252.

Felsenstein J. 1985. Phylogenies and the Comparative Method. *American Naturalist* **125**: 1-15.

Ferrari L, Orozco-Esquivel T, Manea V, Manea M. 2012. The dynamic history of the Trans-Mexican Volcanic Belt and the Mexico subduction zone. *Tectonophysics* **522-523**: 122-149.

Fick SE, Hijmans RJ. 2017. WorldClim 2: new 1-km spatial resolution climate surfaces for global land areas. *International Journal of Climatology* **37**: 4302-4315.

FitzJohn RG. 2012. Diversitree: comparative phylogenetic analyses of diversification in R. *Methods in Ecology and Evolution* **3**: 1084-1092.

Garland T, Harvey PH, Ives AR. 1992. Procedures for the analysis of comparative data using phylogenetically independent contrasts. *Systematic Biology* **41**: 18-32.

Gaut BS, Muse SV, Clark WD, Clegg MT. 1992. Relative rates of nucleotide substitution at the *rbcL* locus of monocotyledonous plants. *Journal of Molecular Evolution* **35**: 292-303.

Goloboff PA, Farris JS, Nixon KC. 2008. TNT, a free program for phylogenetic analysis. *Cladistics* **24**: 774-786.

Govaerts R, Dransfield J. 2005. World checklist of palms. Richmond: Royal Botanic Gardens, Kew.

Govaerts R, Dransfield J, Zona S, Hodel DR, Henderson A. 2018. World Checklist of Arecaceae. Facilitated by the Royal Botanic Gardens, Kew. Published on the Internet; http://wcsp.science.kew.org/ Retrieved 16 August 2018.

Harvey PH, MD Pagel. 1991. The comparative method in evolutionary biology. Oxford: Oxford University Press.

Henderson A, Galeano G, Bernal R. 1995. Field guide to the palms of the Americas. Princeton: Princeton University.

Heyduk K, Trapnell DW, Barrett CF, Leebens-Mack J. 2015. Phylogenomic analyses of species relationships in the genus Sabal (Arecaceae) using targeted sequence capture. *Biological Journal of the Linnean Society* **117**: 106-120.

Hijmans RJ, Phillips S, Leathwick J, Elith J. 2017. Dismo: Species Distribution Modeling: R package version 1.1-4. https://cran.r-project.org/package=dismo

Hodel, D. R. 2006. Beautiful *Brahea*. *Palm Journal* **184**: 4-15.

Hodel, D. R. 2018a. An overview of *Brahea*. *Palm Journal* **215**: 4-23.

Jackson ND, Morales AE, Carstens BC, O'Meara BC. 2017. PHRAPL: Phylogeographic inference using approximate likelihoods. *Systematic Biology* **66**: 1045-1053.

Johnson D. 1998. *Brahea edulis*. The IUCN Red List of Threatened Species 1998: e.T38455A10120521. http://dx.doi.org/10.2305/IUCN.UK.1998.RLTS.T38455A10120521.en.

Katoh K, Standley DM. 2013. MAFFT Multiple sequence alignment software version 7: Improvements in performance and usability. *Molecular Biology and Evolution* **30**: 772-780.

Klimova A, Hoffman JI, Gutierrez-Rivera JN, de la Luz JL, Ortega-Rubio A. 2017. Molecular genetic analysis of two native desert palm genera, *Washingtonia* and *Brahea*, from the Baja California Peninsula and Guadalupe Island. *Ecology and Evolution* **7**: 4919-4935.

Kubatko LS, Degnan JH. 2007. Inconsistency of phylogenetic estimates from concatenated data under coalescence. *Systematic Biology* **56**: 17-24.

Lanfear R, Ho SYW, Davies TJ, *et al*. 2013. Taller plants have lower rates of molecular evolution. *Nature Communications* **4:** 1879.

Martius CFP. 1838. *Historia Naturalis Palmar* **3**: 243-244.

Matzke NJ. 2014. Model selection in historical biogeography reveals that founder-event speciation is a crucial process in island clades. *Systematic Biology* **63**: 951-970.

Moore HE. 1973. The major groups of palms and their distribution. *Gentes Herbarum* **11**: 27-140.

Morales AE, Jackson ND, Dewey TA, O'Meara BC, Carstens BC. 2017. Speciation with gene flow in North American *Myotis* bats. *Systematic Biology* **66**: 440-452.

Nunes LA, Pearson RG. 2017. A null biogeographical test for assessing ecological niche evolution. *Journal of Biogeography* **44**: 1331-1343.

Pan AD, Jacobs BF, Dransfield J, Baker WJ. 2006. The fossil history of palms (Arecaceae) in Africa and new records from the Late Oligocene (28–27 Mya) of north-western Ethiopia. *Botanical Journal of the Linnean Society* **151**: 69-81.

Paradis E, Claude J, Strimmer K. 2004. APE: Analyses of Phylogenetics and Evolution in R

764 language. *Bioinformatics* **20**: 289-290.
765 **Phillips SJ, Anderson RP, Dudik M, Schapire RE, Blair ME. 2017.** Opening the black box:
766 an open-source release of Maxent. *Ecography* **40**: 887-893.
767 **Pulido MT, Coronel-Ortega M. 2015.** Ethnoecology of the palm *Brahea dulcis* (Kunth) Mart.
768 in central Mexico. *Journal of Ethnobiology and Ethnomedicine* **11**: 1-17.
769 **Pyron RA, Costa GC, Patten MA, Burbrink FT. 2015.** Phylogenetic niche conservatism and
770 the evolutionary basis of ecological speciation. *Biological Reviews* **90**: 1248-1262.
771 **Quero H. 2000**. *Brahea sarukhanii*, a new species of palm from Mexico. *Palms* **44**: 103-119.
772 **Quero H, Yáñez E. 2000**. El complejo *Brahea-Erythea* (Palmae: Coryphideae). Proyecto
773 CONABIO L216. Informe final. http://www.conabio.gob.mx/institucion/cgi-
774 bin/datos.cgi?Letras=L&Numero=216 [accessed 20 October 2010]
775 **R Core Team. 2016.** R: A language and environment for statistical computing. R Foundation for
776 Statistical Computing, Vienna, Austria. URL https://www.R-project.org/
777 **Rambaut A, Drummond AJ, Xie D, Baele G and Suchard MA. 2018**. Tracer v1.7, Available
778 from http://beast.community/tracer
779 **Ramirez-Rodriguez R, Tovar-Sanchez E, Ramirez JJ, Flores KV, Rodriguez V. 2011.**
780 Introgressive hybridization between *Brahea dulcis* and *Brahea nitida* (Arecaceae) in
781 Mexico: evidence from morphological and PCR-RAPD patterns. *Botany-Botanique* **89**:
782 545-557.
783 **Revell LJ. 2012.** Phytools: an R package for phylogenetic comparative biology (and other
784 things). *Methods in Ecology and Evolution* **3**: 217-223.
785 **Riddle BR, Hafner DJ, Alexander LF, Jaeger JR. 2000**. Cryptic vicariance in the historical
786 assembly of a Baja California peninsular desert biota. *Proceedings of the National*
787 *Academy of Sciences of the United States of America* **97**: 14438-14443.
788 **Robinson DF, Foulds LR. 1979.** Comparison of weighted labeled trees. *Lecture Notes in*
789 *Mathematics* **748**: 119-126.
790 **Ronquist F, Teslenko M, van der Mark P, *et al*. 2012.** MrBayes 3.2: Efficient Bayesian
791 phylogenetic inference and model choice across a large model space. *Systematic Biology*
792 **61**: 539-542.
793 **Sanderson MJ. 1997.** A nonparametric approach to estimating divergence times in the absence
794 of rate constancy. *Molecular Biology and Evolution* **14**: 1218-1231.
795 **Schrank E. 1994**. Palynology of the Yesomma Formation in Northern Somalia: a study of pollen
796 spores and associated phytoplankton from the late Cretaceous Palmae Province.
797 *Palaeontographica Abteilung B* **231**: 63-112.
798 **Sedlock RL, Ortega-Gutierrez F, Speed RC, 1993**. Tectonostratigraphic terranes and tectonic
799 evolution of Mexico. *Geological Society of America Special Papers* **278**: 153 pp.
800 **Stamatakis A. 2014.** RAxML version 8: a tool for phylogenetic analysis and post-analysis of
801 large phylogenies. *Bioinformatics* **30**: 1312-1313.
802 **Swofford D. 2002.** PAUP Version 4.0. Phylogenetic Analysis Using Parsimony (and other
803 methods). Sunderland: Sinauer Associates, Inc.

804 **Thayer WN. 1916.** The physiography of Mexico: *Journal of Geology* **25**: 61-94.
805 **Uhl NW, Dransfield J. 1987**. Genera Palmarum. Lawrence: Allen Press.
806 **Uhl NW, Dransfield J, Davis JI, Luckow MA, Hansen KS, Doyle JJ. 1995.** Phylogenetic
807 relationships among palms: cladistic analyses of morphological and chloroplast DNA
808 restriction site variation. In: Rudall PJ, Cribb PJ, Cutler DF, Humphries CJ, eds.
809 *Monocotyledons: systematics and evolution*. Kew: Royal Botanic Gardens, Kew, 623-
810 661.
811 **Warren DL, Glor RE, Turelli M. 2008.** Environmental niche equivalency versus conservatism:
812 quantitative approaches to niche evolution. *Evolution* **62**: 2868-2883.
813 **Warren DL, Cardillo M, Rosauer DF, Bolnick DI. 2014.** Mistaking geography for biology:
814 inferring processes from species distributions. *Trends in Ecology & Evolution* **29**: 572-
815 580.
816 **Watson S. 1880.** *Botany of California* **2**: 211.
817 **Wehncke EV, López-Medellín X, Wall M, Ezcurra E. 2013**. Revealing an endemic
818 herbivore-palm interaction in remote desert oases of Baja California. *American Journal*
819 *of Plant Sciences* **4**: 470-478.
820

821

822 **Table 1**. Voucher information and characteristics of high-throughput sequence datasets. HBG =
823 Huntington Botanical Garden live collection; HNT = Huntington Botanical Garden Herbarium;
824 CSLA = California State University, Los Angeles Herbarium; UCBG = UC, Berkeley Botanical
825 Garden live collection; UC = UC, Berkeley & Jepson Herbaria; 'Plastid,' 'rDNA,' and 'mt' =
826 mean coverage depth of the plastome, partial rDNA cistron (18S-ITS-26S), and mitochondrial
827 genomes, respectively. [a]Recognized as a synonym of *B. dulcis* (Hodel, 2006; Govaerts et al.,
828 2018).
829

Species	**Voucher**	**Total # reads**	**Plastid**	**rDNA**	**mt**	**Sequencing**
Chamaerops humilis L.	HBG 2073; HNT 10471	8,677,266	96.6	508.8	10.7	HiSeq2000
Washingtonia robusta H.Wendl.	CSLA Barrett 310 CSLA	37,162,404	1,128.0	2,096.3	176	HiSeq2000
Brahea aculeata (Brandegee) H.E.Moore	HBG 16448; HNT 13042	5,529,618	175.2	2,716.6	18	MiSeq
Brahea armata S.Watson	HBG 23437; HNT 13222	7,273,550	301.3	3,848.1	19.6	MiSeq
Brahea "berlandieri" Bartlett[a]	HBG 28812; HNT 1745	5,051,496	100.6	529.6	29.8	MiSeq
Brahea brandegeei (Purpus) H.E.Moore	HBG 89871; HNT 13043	9,873,046	281.2	4,185.6	16.5	HiSeq2000
Brahea decumbens Rzed.	HBG 35650; HNT 13038	4,013,662	36.2	276.2	9.5	MiSeq
Brahea dulcis (Kunth) Mart.	HBG 23220; HNT 13044	15,361,806	638.2	1,772.7	66.1	NextSeq500
Brahea edulis H.Wendl. ex S.Watson	UCBG 2003.0149; 1869963, UC 1971077	18,933,406	554.7	3,626.7	42.1	HiSeq2500
Brahea moorei L.H.Bailey ex H.E.Moore	UCBG 88.0345; UC 197077	3,103,380	59.3	1,160.6	9.3	MiSeq
Brahea calcarea Liebm. (syn. *B. nitida* André)	HBG 27970; HNT 10472	12,865,552	494.2	871.2	30.1	NextSeq500
Brahea pimo Becc.	HBG 52194; HNT 13045	6,518,544	42.8	615.3	11.4	MiSeq
Brahea salvadorensis H.Wendl. ex Becc.	HBG 35754; HNT 1029	4,917,552	142.8	439.2	20.8	MiSeq
Brahea sarukhanii H.J.Quero	HBG 25151; HNT 10470	15,333,496	279.8	1,617.1	29	NextSeq500

Table 2. Characteristics of the nuclear, mitochondrial, and plastid datasets for *Brahea*. 'Total L' = total length of each alignment; 'post-filter L' = length of each alignment after filtering; '# P-inf sites' = the number of parsimony informative sites; 'P-inf/1000bp' = the number of parsimony informative sites per 1,000 bp of alignment; '#MPT, L' = the number of most parsimonious trees and their length in steps (i.e. number of nucleotide changes); 'model' = the best fit model for each alignment based on the corrected Akaike Information Criterion.'

Locus	total L	post-filter L	# P-inf sites	P-inf/1000bp	#MPT; L	model
MS	601	n/a	18	30.0	9, 41	T92+G
CISP4	664	n/a	22	33.1	3, 60	GTR+G
RPB2	701	n/a	19	27.1	1, 47	HKY+G
rDNA	6,180	n/a	60	9.7	3, 218	TN93+G
Total nrDNA	8,146	7,967	119	14.6	1, 384	TN93+G
mtDNA	261,650	212,874	304	1.2	1, 1,164	GTR+G+I
Plastome	132,870	121,301	333	2.5	1, 938	HKY+G+I
Combined	402,666	342,142	756	2.2	1, 2,490	GTR+G+I

838 **Table 3**. Results of Warren's Identity Test (*I*) run for 1,000 replicates using both the WorldClim
839 and Pearson-Filtered data sets ($\alpha \leq 0.0166$ for the *B. armata* clade, post-Bonferroni correction).

Species Comparison	*I* statistic	P-Value
B. armata vs. *aculeata*	0.249853356	1.44×10^{-45}
B. armata vs. *brandegeei*	0.264126907	5.00×10^{-23}
B. aculeata vs. *brandegeei*	0.126009409	6.02×10^{-15}
B. dulcis vs. "*berlandieri*"	0.179367929	7.09×10^{-64}

840

841

SUPPLEMENTARY INFORMATION

Supplementary Link 1 contains MaxEnt outputs of replicated SDMs for *Brahea aculeata*, *B. armata*, *B. berlandieri*, *B. brandegeei*, and *B. dulcis*. Each folder contains an HTML document named 'maxent.html,' which details all results generated by MaxEnt for each species. Link: https://drive.google.com/file/d/1o0Gp-9y7rk2Ou3xVQ7IUelGBaflhZxjb/view?usp=sharing.

ACKNOWLEDGEMENTS

We thank the staff at the Huntington Library, Art Collections and Botanical Gardens and the University of California Botanical Garden (Holly Forbes) for assistance in collecting material and voucher information. We thank the staff at Global Biologics, LLC. (Sean Blake), Laragen, Inc. (Jinliang Li, Lindy Him), the WVU Genomics Core Facility (Sandy Simon, Ryan Percifield), and the WVU-Marshall Shared Sequencing Facility (Don Primerano, Jun Fan) for sequencing assistance. Financial support was provided by the California State University Program for Education & Research in Biotechnology, and the WVU Program to Stimulate Competitive Research. We thank two anonymous reviewers for their comments improving the manuscript.

FIGURE LEGENDS

Fig. 1. Maximum Likelihood trees based on plastid (**A**), mitochondrial (**B**), nuclear (**C**), and combined (**D**) data. Numbers adjacent to branches are Parsimony Jackknife, Maximum Likelihood Bootstrap, and Bayesian posterior probabilities. '*' = 100% support (or posterior probability = 1 for Bayesian Analysis). '--' = differing topology from ML tree for Parsimony or Bayesian Analysis. Scale bar = substitutions/site.

Fig. 2. Divergence time estimates for *Brahea* based on four fossil calibrations. Scale bar = millions of years before present. Gray bars on nodes = 95% highest posterior density of divergence time estimates; numbers at nodes are mean divergence time estimates. "*" indicates that *B. moorei* is placed in subgenus *Erythea* based on our phylogenetic results, and not in subgenus *Brahea* as in previous treatments.

Fig. 3. Biogeographic reconstruction of ancestral ranges for *Brahea* under BayAreaLike and BayAreaLike+j models in BioGeoBEARS. **A**. Chronogram with most likely ancestral ranges. Numbers adjacent to pie charts indicate the likelihood of the most likely ancestral range (top BayAreaLike, bottom, BayAreaLike+j). Dotted line indicates the approximate dates of origin of Guadalupe Island and the formation of the Gulf of California (7.2 mya). **B**. *Brahea armata* (Santa Barbara, California, USA). **C**. *Brahea dulcis* (Fairchild Tropical Botanical Gardens, Coral Gables, Florida, USA). **D**. *Brahea sarukhanii* (Montgomery Botanical Center, Coral Gables, Florida, USA). Photos: C. Barrett. **E**. Map of Mexico and Central America displaying the six different areas chosen to represent of the range of *Brahea*: A. Baja California; B. Northwestern Mainland Mexico; C. Northeastern Mexico; D. Central/Southern Mexico; E. Southeastern Mexico/Central America; F. Guadalupe Island. Geological events (circles): "**I**." Formation of the Mexican Transvolcanic Belt (15 mya onward); "**II**." Opening of the Gulf of California (7.2 mya onward); "**III**." Formation of Guadalupe Island (7.2 mya).

Fig. 4. ML ancestral state reconstruction of maximum height among species of *Brahea*, based on a Brownian Motion model in the R packages 'APE' and 'PhyTools." Numbers at tips are maximum height values (in meters), and at nodes these are ancestral estimates of maximum height, with one standard error in parentheses. "*" indicates the two dwarf forms.

A. Complete Plastome

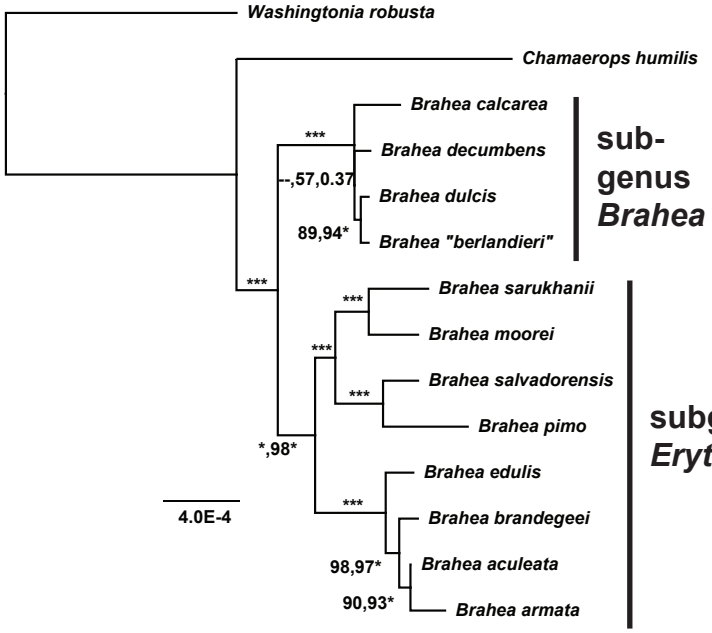

B. Mitochondrial DNA

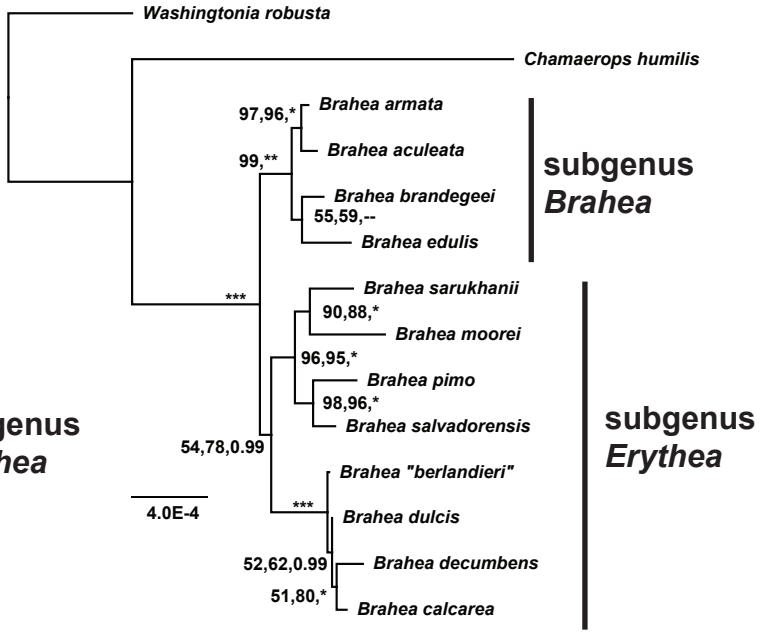

C. Combined Nuclear DNA

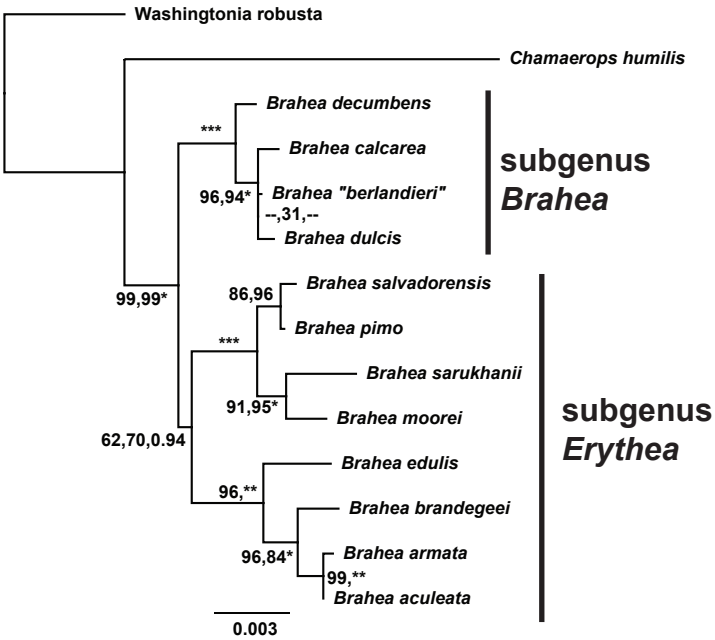

D. All Data Combined

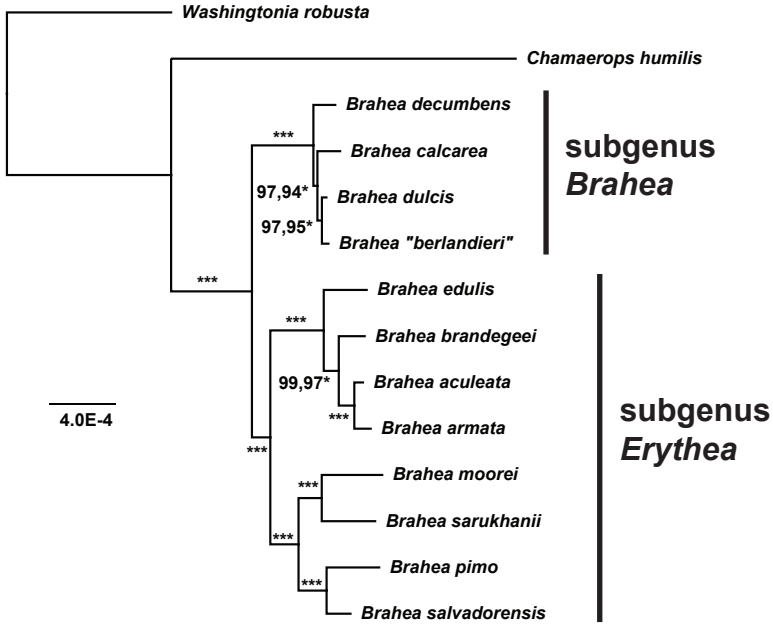

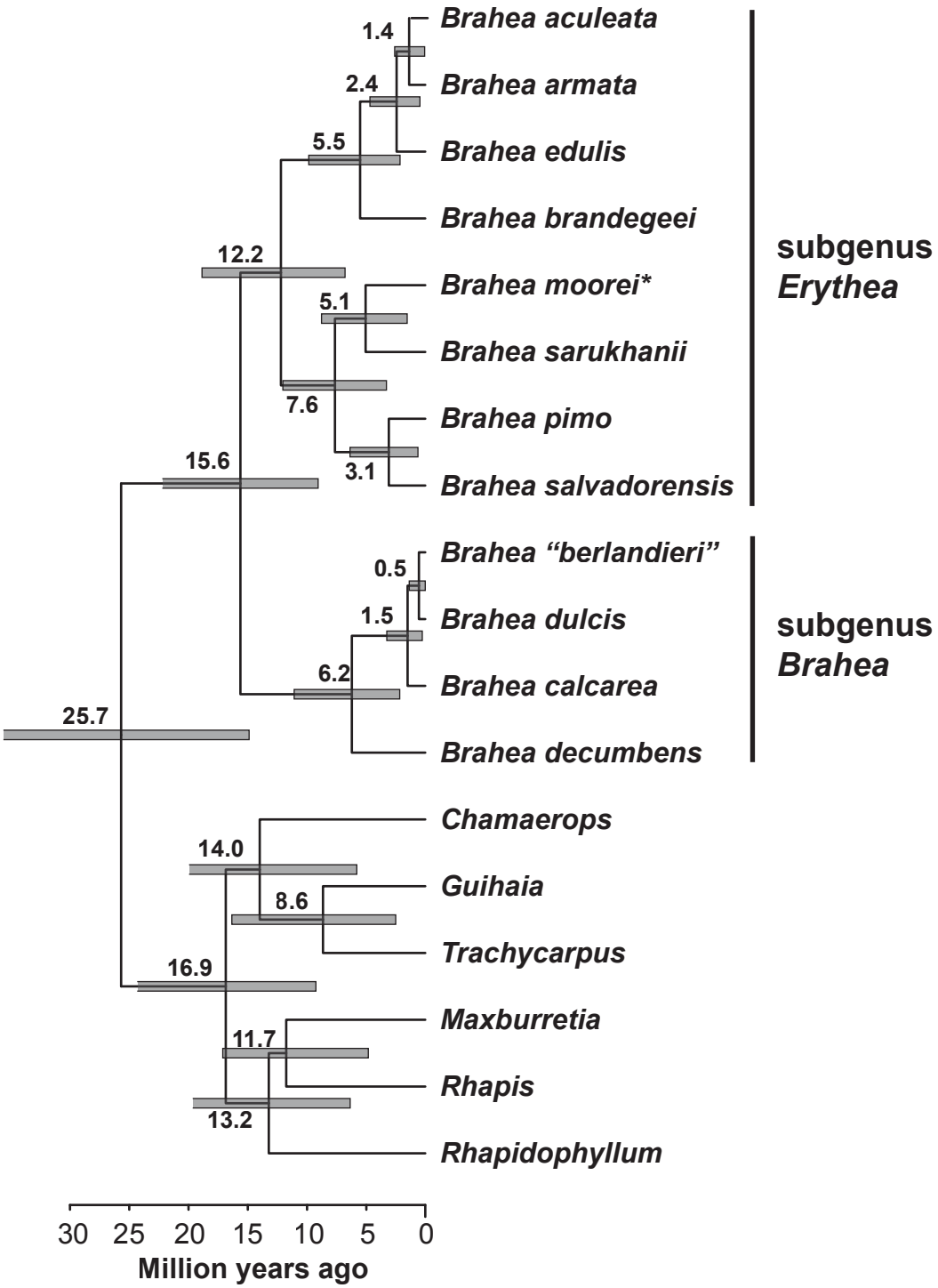

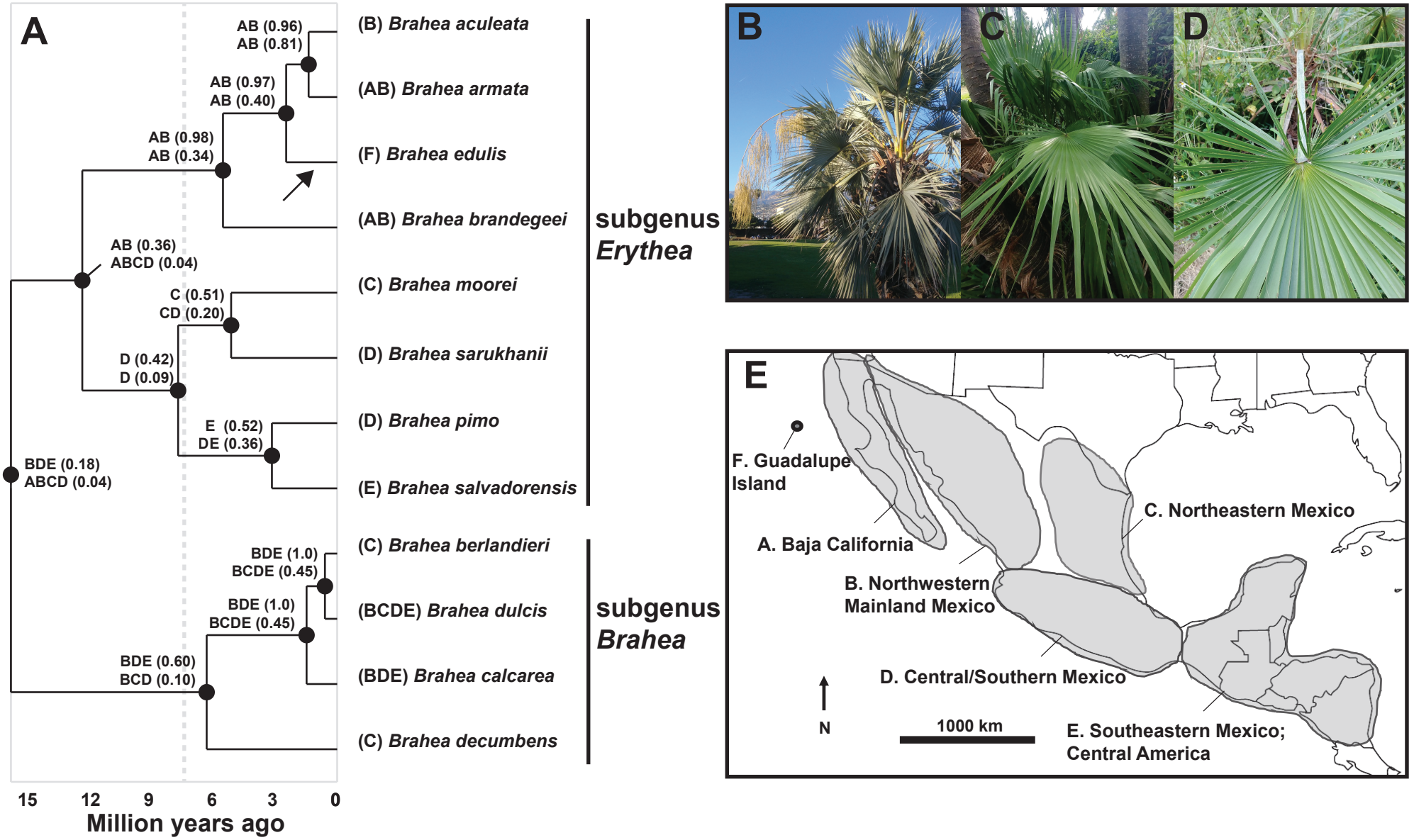
A
AB (0.96)
AB (0.81)
AB (0.97)
AB (0.40)
AB (0.98)
AB (0.34)
AB (0.36)
ABCD (0.04)
C (0.51)
CD (0.20)
D (0.42)
D (0.09)
E (0.52)
DE (0.36)
BDE (0.18)
ABCD (0.04)
BDE (1.0)
BCDE (0.45)
BDE (1.0)
BCDE (0.45)
BDE (0.60)
BCD (0.10)
15
12
9
6
3
0
Million years ago
(B) Brahea aculeata
(AB) Brahea armata
(F) Brahea edulis
(AB) Brahea brandegeei
(C) Brahea moorei
(D) Brahea sarukhanii
(D) Brahea pimo
(E) Brahea salvadorensis
(C) Brahea berlandieri
(BCDE) Brahea dulcis
(BDE) Brahea calcarea
(C) Brahea decumbens
subgenus Erythea
subgenus Brahea
B
C
D
E
F. Guadalupe Island
A. Baja California
B. Northwestern Mainland Mexico
C. Northeastern Mexico
D. Central/Southern Mexico
E. Southeastern Mexico; Central America
N
1000 km